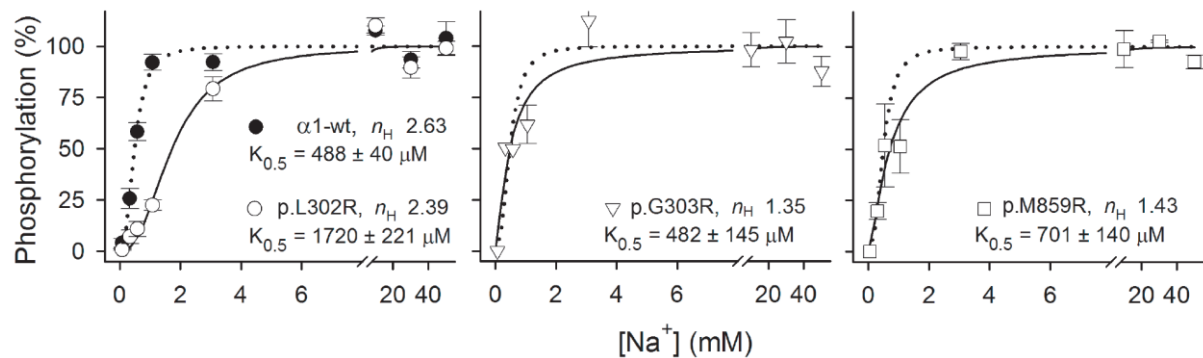


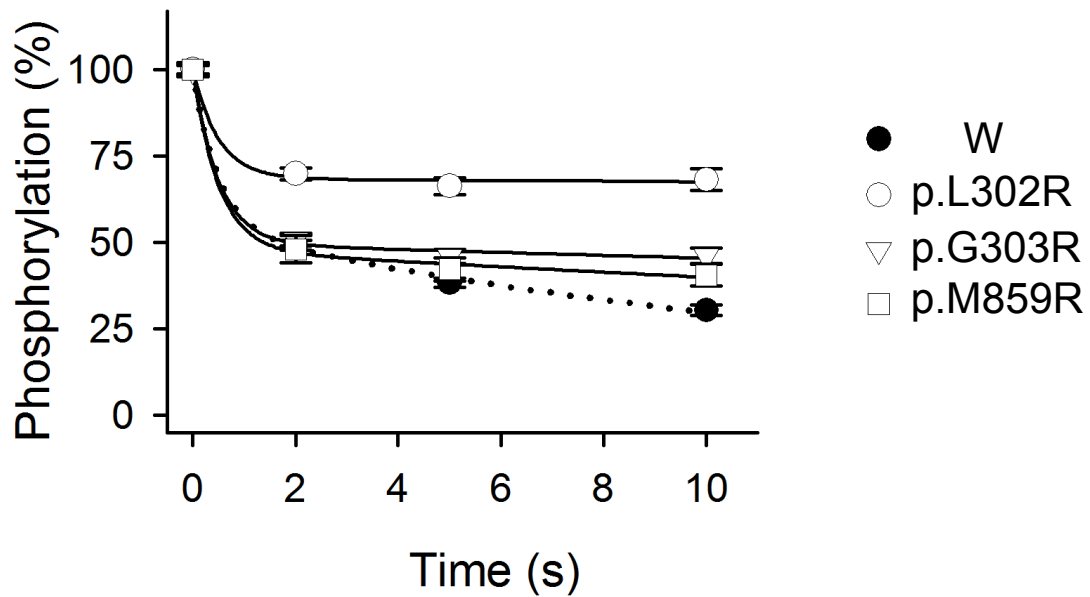
## SUPPLEMENTAL DATA

FIGURE S1:



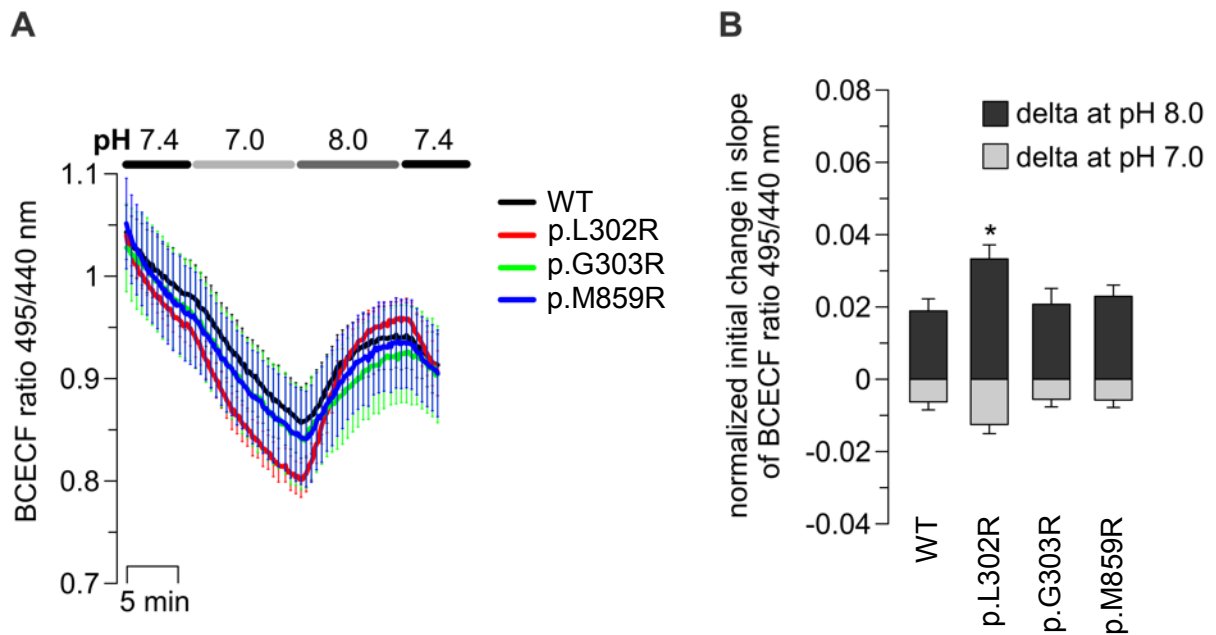
**Figure S1: The Na<sup>+</sup> dependence of phosphorylation from figure 2C shown in separate panels for the three mutants with statistics.** Error bars indicate SEM for the independent experimental points ( $n = 4-5$ ). The indicated Hill coefficients ( $n_H$ ) and  $K_{0.5}$  values with SEM values were obtained by fitting the Hill equation <sup>1</sup> to the data, resulting in the lines shown. The 3.5-fold loss of affinity (reduced  $K_{0.5}$ ) for p.Leu302Arg (p.L302R) is significant ( $p < 0.001$  using one-way ANOVA test). The obtained Hill coefficients indicate WT-like cooperativity of Na<sup>+</sup> binding for p.Leu302Arg (p.L302R), whereas cooperativity was lost for p.Gly303Arg (p.G303R) and p.Met859Arg (p.M859R), as also indicated by the crossing of the line representing the mutant with that of the wild type (WT shown by dotted line in all panels).

FIGURE S2:



**Figure S2: Dephosphorylation of the Na/K-ATPase phosphoenzyme upon addition of ADP for the determination of the distribution of Na<sup>+</sup>-bound E1P and the K<sup>+</sup>-sensitive E2P form:** The amplitude of the rapid phase of dephosphorylation was either WT-like (p.Gly303Arg (p.G303R) and p.Met859Arg (p.M859R)) or reduced in size (p.Leu302Arg (p.L302R)) indicating the presence of more E2P than seen for the WT. These data (n = 13-26) indicate that the reduced K<sup>+</sup> sensitivity observed for all mutants (see figure 2D), is due to a direct effect on K<sup>+</sup> interaction with the E2P state and not caused indirectly by a shift of the E1P-E2P distribution in favor of the K<sup>+</sup>-insensitive E1P.

FIGURE S3:



**Figure S3: Influence of extracellular pH changes on intracellular pH in adrenal NCI-H295R cells expressing wildtype (WT) or different mutant (p.Leu302Arg (p.L302R), p.Gly303Arg (p.G303R), p.Met859Arg (p.M859R)) ouabain-insensitive rat *Atp1a1*.** Cells were analysed 2 days after transient transfection with *Atp1a1* containing bicistronic plasmids using electroporation. Transfected cells were identified using anti-CD8 coated dynabeads and compared to untransfected cells (devoid of beads) from the same dish. The pH of the extracellular solution was changed from control pH 7.4 to pH 7.0, followed by pH 8.0. The intracellular pH was measured using the pH-sensitive BCECF dye. BCECF ratios (495/440 nm), normalized to the baseline pH of untransfected cells, are shown in (A) indicating intracellular acidification by a decreased ratio and alkalization by an increased ratio, respectively. Expression of the p.Leu302Arg mutant (n=10) led to stronger changes of the intracellular pH upon altering the extracellular pH, whereas p.Gly303Arg (n=7) and p.Met859Arg (n=7) mutant cells were not different from WT cells (n=8). (B) Reactivity of the intracellular pH to alterations of the extracellular pH was quantified by calculating the initial changes in the slope of the BCECF ratio (given here as delta of slope at pH 7.0 and 8.0 compared to the

slope at the end of the pH7.4 control). \* $p < 0.05$  compared to WT at pH 8.0; n is equal to the number of dishes (measured from different cell passages and at different days of experiments).

SUPPLEMENTAL METHODS AND RESULTS:

PATIENTS

Table S1:

Individual	A-II-1	B-II-1	C-II-2
Origin	of European descent	of European descent	First Nations Canadian
Gender	female	female	male
Age at manifestation	6 months	2 months	6 days
First symptom	generalized seizures	generalized seizures	generalized seizures
<u>Initial laboratory findings:</u>			
S-Na (mmol/L) (136-144)	135	139	141
S-K (mmol/L) (3.6-5.2)	3.8	4.2	2.1
S-Ca (mmol/L) (2.1-2.6)	2.24	2.58	0.9 (ionized, 1.05-1.35)
S-Mg (mmol/L) (0.75-1.1)	0.36	0.35	0.30
S-HCO <sub>3</sub> (mmol/L) (22-26)	26.7	22.0	27.0
Ca/Crea-ratio (mol/mol) (<2.2)	0.24	0.46	4.95
FE-Mg (%) (3-5%)	26.0	33.8	nd
<u>Actual laboratory findings:</u>			
S-Na (mmol/L) (136-144)	136	140	139
S-K (mmol/L) (3.6-5.2)	3.3	3.0	3.9
S-Ca (mmol/L) (2.1-2.6)	2.52	2.23	2.13
S-Mg (mmol/L) (0.75.-1.1)	0.57	0.28	0.62
S-HCO <sub>3</sub> (mmol/L) (22-26)	26.3	25.0	22.0
Ca/Crea-ratio (mol/mol) (<0.9)	0.41	0.40	0.44

FE-Mg (%) (3-5%)	15.3	27.0	21.3
nephrocalcinosis	no	no	no
arterial hypertension	no	no	No
cardiac examination <sup>a</sup>	normal	n.d.	normal
renin (ng/L) (5-67)	53ng/L	n.d.	n.d.
PRA <sup>b</sup> (ng/mL/h) (<7)	n.d.	15.5	1.33
aldosterone (ng/dL) (1-40)	5.2	11.2	1.8
ADRR <sup>c</sup> /ARR <sup>d</sup> (<30)	1.0 (ADRR)	0.7 (ARR)	1.4 (ARR)
seizure activity	repeated status epilepticus	monthly seizures	frequent seizures, repeated status epilepticus
cerebral imaging (MRI)	initially normal, cerebral volume loss during follow-up	normal	mild ventriculomegaly, incomplete myelination
neurological outcome	global developmental delay, hyperactive behavior	global developmental delay, suspected autism spectrum disorder	global developmental delay, speech delay, diagnosis of severe autism, self-biting behaviour
<u>ATP1A1 mutations</u>			
- nucleotide level	c.905T>C	c.907G>C	c.2576T>G
- protein level	p.Leu302Arg	p.Gly303Arg	p.Met859Arg

<sup>a</sup> by electrocardiogram and echocardiography, <sup>b</sup> PRA = plasma renin activity, <sup>c</sup> ADRR = aldosterone-direct renin-ratio, <sup>d</sup> ARR = aldosterone-renin activity-ratio,

Table S1: Clinical Characteristics and Genotypes (complete dataset).

## SEQUENCING

The family C trio as well as individual A-II-1 were subjected to whole exome sequencing in separate studies.

Family C was enrolled within the TIDEX gene discovery project (H12-00067), which was approved by the Research Ethics Board of BC Children's and Women's Hospital, University of British Columbia, Vancouver, Canada. Whole exome sequencing was performed for the affected child (C-II-2), mother (C-I-2), and father (C-I-1) of family C. C-II-2 was sequenced using the Agilent SureSelectXT kit and Illumina HiSeq 4000 (Macrogen, South Korea). Mother and father were sequenced using the Agilent V4 51Mb kit and Illumina HiSeq 2000 (Perkin-Elmer, CA, USA). The sequence data was processed and analyzed using a semi-automated pipeline as previously reported <sup>2</sup>. Sequencing reads were aligned to the hg19 human reference genome. Rare variants were assessed for predicted functional impact, using CADD, SIFT and PolyPhen, and were screened under multiple inheritance models. For patient C-II-2, homozygous variants in 9 genes, compound-heterozygous variants in 6 genes, hemizygous variants in 3 genes, and *de-novo* variant in 1 gene were identified.

Singleton exome sequencing of individual A-II-1 was performed from 200ng of genomic DNA. Target enrichment was carried out using the standard protocol SureSelectXT Automated Target Enrichment for Illumina paired-end multiplexed sequencing, and the Agilent Bravo automated liquid handling platform <sup>3</sup>. After validation (2200 TapeStation; Agilent Technologies, CA, USA) and quantification (Qubit System; Invitrogen, Waltham, MA, USA), 2x75 bp paired-end reads were sequenced on a HiSeq 4000 (Illumina, San Diego, California). For data analysis, the VARBANK pipeline v.2.15 (unpublished) and the corresponding filter interface was used. Sequence reads were mapped to the hg19/GRCh37 human reference

genome using the Burrows Wheeler Aligner (BWA) alignment algorithm with a mean target coverage of 80 reads per base and 82.4% of targeted bases covered more than 30x.

In individual A-II-1, 4 genes with homozygous variants and 4 genes with more than one potentially pathogenic variant were identified. In addition, the data analysis of individual A-II-1 revealed heterozygous variants in 310 genes.

Comparison of exome data from the two affected individuals (A-II-1 and C-II-2) demonstrated no additional shared gene, beyond *ATP1A1*, with homozygous, compound-heterozygous, or de-novo mode of inheritance. Finally, we also could not identify a gene with a rare heterozygous variant shared by both individuals (A-II-1 and C-II-2).

In contrast, both individuals were found to carry a single heterozygous mutation, p.Leu302Arg and p.Met859Arg in *ATP1A1*, respectively. Targeted Sanger sequencing of index, mother, father and unaffected sibs for family A and C confirmed that both variants occurred *de-novo*. Subsequently, conventional Sanger sequencing of the entire coding region and adjacent exon/intron boundaries of *ATP1A1* revealed a third heterozygous mutation, p.Gly303Arg, in individual B-II-1 that also occurred *de-novo* (see Table S1).

Table S2:

Gene	Individual	Nucleotide change (hg19, cDNA)	Protein change (AA)	Inheritance	SIFT (score)	Polyphen2 (score)
<i>ATP1A1</i>	A-II-1	chr1:116932211 T>G c.905T>G	p.Leu302Arg	heterozygous, <i>de-novo</i>	damaging 0.000	probably damaging 0.985
<i>ATP1A1</i>	B-II-1	chr1:116932213 G>C c.907G>C	p.Gly303Arg	heterozygous, <i>de-novo</i>	damaging 0.000	probably damaging 1.000
<i>ATP1A1</i>	C-II-2	chr1:116943486 T>G c.2576T>G	p.Met859Arg	heterozygous, <i>de-novo</i>	damaging 0.013	possibly damaging 0.561

(RefSeq NM\_000701, NP\_000692, Transcript ID ENST00000295598, UniProt P05023)

**Table S2: Mutations in *ATP1A1*.** In silico analyses predicted the variants to be pathogenic (p.Leu302Arg: CADD<sup>4</sup> (32.0); SIFT<sup>5</sup> (Damaging; 0.000); Polyphen2<sup>6</sup> (Probably damaging; 0.985); p.Gly303Arg: CADD (31.0); SIFT (Damaging; 0.000); Polyphen2 (Probably damaging; 1.000); p.Met859Arg: CADD (24.6); SIFT (Damaging; 0.013); PolyPhen2 (Possibly damaging; 0.561)), affecting highly conserved amino acid residues of the Na/K-ATPase  $\alpha$ 1 protein. None of the identified mutations are listed in publically available exome or genome databases, i.e. ExAC browser ([exac.broadinstitute.org](http://exac.broadinstitute.org)) or Genome Aggregation Database (gnomAD) (<http://gnomad.broadinstitute.org/>).

## MEASUREMENT OF Na/K-ATPase ACTIVITY

For biochemical studies, mutations were introduced into full-length cDNA encoding the ouabain insensitive rat  $\alpha$ 1-isoform of Na/K-ATPase. COS-1 cells were used to express the mutants and wild type, either by the ouabain selection method <sup>7</sup>, attempting to obtain stable viable cell lines, or by transient expression in the presence of siRNA to knock down endogenous Na/K-ATPase <sup>8</sup>. Leaky plasma membranes were assayed functionally by previously described methods <sup>1</sup>. Phosphorylation was carried out for 10 s at 0°C with 2  $\mu$ M [ $\gamma$ -<sup>32</sup>P]ATP in the presence of varying concentrations of NaCl (100 mM for maximum phosphorylation), 3 mM MgCl, 20 mM Tris (pH 7.5), 100  $\mu$ M ouabain, and 20  $\mu$ g oligomycin/ml, or in the presence of 50 mM NaCl, 3 mM MgCl, 20 mM Tris (pH 7.5), 100  $\mu$ M ouabain, and varying concentrations of KCl with choline chloride added to maintain a constant ionic strength.

For determination of the E1P-E2P-distribution the phosphorylation was carried out in the absence of KCl and dephosphorylation was followed by quenching at various time intervals after addition of 2.5 mM ADP with 1 mM unlabeled ATP. In all phosphorylation experiments the radioactively labeled Na/K-ATPase was separated by acid SDS gel electrophoresis following acid quenching of the reaction mix, and the radioactivity quantified by phosphor imaging.

## FUNCTIONAL STUDIES

Plasmids containing full-length cDNA sequences encoding wild-type or mutant ouabain-insensitive rat *Atp1a1* were generated as described <sup>8,9</sup>. Adrenocortical carcinoma NCI-H295R cells (CLS) were transfected using electroporation as described <sup>9</sup>. Cells were analyzed 48

hours after transfection. For patch-clamp, pH, and  $\text{Ca}^{2+}$  measurements, transfected cells were identified using anti-CD8-coated dynabeads (Life Technologies GmbH).

Whole-cell patch recordings were performed at room temperature using an EPC 10 amplifier (Heka), relative cytosolic pH levels were measured using the ratiometric fluorescent pH sensitive dye BCECF-AM (Life Technologies GmbH) as described <sup>9</sup>. For  $\text{Na}^+$ -free extracellular conditions, bath  $\text{Na}^+$  was replaced by N-methyl-D-glucamine ( $\text{NMDG}^+$ ). In addition, flame photometry was used for the determination of intracellular  $\text{Na}^+$  and  $\text{K}^+$  contents as described <sup>10</sup>. Intracellular  $\text{Na}^+$  and  $\text{K}^+$  contents were measured under control conditions and after treatment with 10  $\mu\text{M}$  ouabain inhibiting endogenous human ATP1A1 but not the transfected ouabain-insensitive rat ATP1A1. Cultured cells were washed with a  $\text{Na}^+$ -free solution before swelling and disruption of cells was induced by incubation in MilliQ-water on ice for 1.5 hours. Cell lysates are homogenized mechanically and cleared from cellular debris by centrifugation. Finally,  $\text{Na}^+$ - and  $\text{K}^+$  concentrations in the supernatant were measured using flame photometry (PFP7 Industrial Flame Photometer, Jenway/Cole Parmer, Staffordshire, UK). Ion concentrations were calculated as ratios of  $\text{Na}^+$ - or  $\text{K}^+$  content, respectively, compared to the sum of  $\text{Na}^+$  and  $\text{K}^+$  content.

#### STATISTICAL ANALYSIS

Phosphorylation data were analyzed using the SigmaPlot program (SPSS, Inc.) for non-linear regression using the Hill equation for cooperative binding <sup>1</sup>. Statistical significance was tested using Student's t test (for paired or unpaired samples as appropriate). All data are presented as mean  $\pm$  SEM. For multiple comparisons, an ANOVA plus Bonferroni or Holm-Sidak post-hoc test was used. Differences between groups were considered significant if  $p < 0.05$  for single comparisons or  $p < 0.01$  for multiple comparisons.

## LITERATURE

1. Toustrup-Jensen, M.; Hauge, M.; Vilsen, B., Mutational effects on conformational changes of the dephospho- and phospho-forms of the Na<sup>+</sup>,K<sup>+</sup>-ATPase. *Biochemistry* **2001**, *40* (18), 5521-32.
2. Tarailo-Graovac, M.; Shyr, C.; Ross, C. J.; Horvath, G. A.; Salvarinova, R.; Ye, X. C.; Zhang, L. H.; Bhavsar, A. P.; Lee, J. J.; Drogemoller, B. I.; et al., Exome Sequencing and the Management of Neurometabolic Disorders. *N Engl J Med* **2016**, *374* (23), 2246-55.
3. Altmuller, J.; Motameny, S.; Becker, C.; Thiele, H.; Chatterjee, S.; Wollnik, B.; Nurnberg, P., A systematic comparison of two new releases of exome sequencing products: the aim of use determines the choice of product. *Biol Chem* **2016**, *397* (8), 791-801.
4. Kircher, M.; Witten, D. M.; Jain, P.; O'Roak, B. J.; Cooper, G. M.; Shendure, J., A general framework for estimating the relative pathogenicity of human genetic variants. *Nat Genet* **2014**, *46* (3), 310-5.
5. Ng, P. C.; Henikoff, S., Predicting deleterious amino acid substitutions. *Genome Res* **2001**, *11* (5), 863-74.
6. Adzhubei, I. A.; Schmidt, S.; Peshkin, L.; Ramensky, V. E.; Gerasimova, A.; Bork, P.; Kondrashov, A. S.; Sunyaev, S. R., A method and server for predicting damaging missense mutations. In *Nat Methods*, United States, 2010; Vol. 7, pp 248-9.
7. Vilsen, B., Glutamate 329 located in the fourth transmembrane segment of the alpha-subunit of the rat kidney Na<sup>+</sup>,K<sup>+</sup>-ATPase is not an essential residue for active transport of sodium and potassium ions. *Biochemistry* **1993**, *32* (48), 13340-9.
8. Beuschlein, F.; Boulkroun, S.; Osswald, A.; Wieland, T.; Nielsen, H. N.; Lichtenauer, U. D.; Penton, D.; Schack, V. R.; Amar, L.; Fischer, E.; et al., Somatic mutations in ATP1A1 and ATP2B3 lead to aldosterone-producing adenomas and secondary hypertension. *Nat Genet* **2013**, *45* (4), 440-4, 444e1-2.

9. Stindl, J.; Tauber, P.; Sterner, C.; Tegtmeier, I.; Warth, R.; Bandulik, S., Pathogenesis of Adrenal Aldosterone-Producing Adenomas Carrying Mutations of the Na(+)/K(+)-ATPase. *Endocrinology* **2015**, *156* (12), 4582-91.
  
10. Tauber, P.; Aichinger, B.; Christ, C.; Stindl, J.; Rhayem, Y.; Beuschlein, F.; Warth, R.; Bandulik, S., Cellular Pathophysiology of an Adrenal Adenoma-Associated Mutant of the Plasma Membrane Ca(2+)-ATPase ATP2B3. *Endocrinology* **2016**, *157* (6), 2489-99.